NASA Technical Memorandum 101978

Icing Research Tunnel Test of a Model Helicopter Rotor

Thomas L. Miller
Sverdrup Technology, Inc.
NASA Lewis Research Center Group
Cleveland, Ohio

and

Thomas H. Bond
National Aeronautics and Space Administration
Lewis Research Center
Cleveland, Ohio

Prepared for the
45th Annual Forum and Technology Display
sponsored by the American Helicopter Society
Boston, Massachusetts, May 22–24, 1989

NASA

ICING RESEARCH TUNNEL TEST OF A MODEL HELICOPTER ROTOR

Thomas L. Miller
Sverdrup Technology, Inc.
NASA Lewis Research Center Group
Cleveland, Ohio

and

Thomas H. Bond
National Aeronautics and Space Administration
Lewis Research Center
Cleveland, Ohio

Abstract

An experimental program has been conducted in the NASA Lewis Research Center Icing Research Tunnel (IRT) in which an OH-58 tail rotor assembly was operated in a horizontal plane to simulate the action of a typical main rotor. Ice was accreted on the blades in a variety of rotor and tunnel operating conditions and documentation of the resulting shapes was performed. Rotor torque and vibration are presented as functions of time for several representative test runs, and the effects of various parametric variations on the blade ice shapes are shown. This OH-58 test was the first of its kind in the United States and will encourage additional model rotor icing tunnel testing. Although not a scaled representative of any actual full-scale main rotor system, this rig has produced torque and vibration data which will be useful in assessing the quality of existing rotor icing analyses.

Introduction

Motivated by a desire in recent years to increase their all-weather operational capabilities, U.S. helicopter manufacturers have expressed a need for alternate methods of acquiring rotor icing data to be used in obtaining certification for flight in natural icing conditions. Present certification and rotor icing data acquisition efforts depend very heavily upon flight testing over a wide range of natural icing scenarios, a range which is often seemingly unattainable due to the scarcity of some of the conditions required. So presently helicopter icing certification is a long, difficult, expensive, and potentially dangerous process.

Various efforts have been undertaken in the past in attempting to investigate the causes and effects of rotor ice accretion but few involved scaled airfoil wind tunnel testing. The helicopter companies have conducted limited icing flight tests on their respective aircraft as requirements dictated, but few comprehensive research-oriented programs have taken place. One such program though was the Helicopter Icing Flight Test (HIFT) program, a multi-year effort involving NASA, Bell Helicopter Textron, FluiDyne Engineering Corporation, Hovey and Associates, and The Ohio State University.[1-4] In this full scale flight test program, a UH-1H helicopter was flown in both hover and forward flight at the Ottawa Spray Rig and behind the Army HISS tanker to acquire rotor ice shape data. Horsepower increases in icing were also documented with which analytical predictions of iced rotor performance could be compared. Ice shapes obtained in these tests were also tested in the FluiDyne transonic wind tunnel to determine iced airfoil section drag rises. This gave another measure of iced rotor section performance which could be compared with calculated predictions.

A different approach to the collection of iced rotor performance data has been taken by Texas A&M University.[5,6] In this study, an artificial ice shape was attached to the rotor blades of a model helicopter and the aircraft was then operated in the Texas A&M 7- by 10-ft low speed wind tunnel. Resultant forces and moments were measured to provide a measure of iced rotor performance. Substantial torque rises due to icing were documented and the effect of radial icing extent on iced rotor performance was demonstrated. Although additional validation of this type of testing is required, it demonstrated that iced rotor performance data could indeed be obtained by this method.

The only icing wind tunnel testing of a model rotor conducted prior to the OH-58 Tail Rotor Rig test was performed by the French.[7] A 1/4 scale model rotor was tested in the ONERA SIMA wind tunnel at Modane, France. The effects of various parameters including velocity, droplet diameter, static temperature, and liquid water content on the resulting ice accretion were studied and an electrothermal de-icing system incorporated into the blade was operated to obtain scaled de-icing system data. The French feel that this ice accretion and performance data compared favorably with full-scale natural icing flight test data, thereby indicating that this method is a viable way of collecting iced rotor data, although the scaled de-icer data is of questionable quality.

In response to the need expressed by the U.S. helicopter manufacturers, NASA Lewis has undertaken a program to demonstrate the usefulness of the Icing Research Tunnel as a facility for obtaining meaningful icing data for rotating systems. The range and controllability of conditions in the tunnel make it a powerful tool for study of the effects of ice accretion on rotors and propellers. This paper will detail the testing of the OH-58 Tail Rotor Rig, the first model rotor to be tested in the IRT, and illustrate

the viability of using the IRT for conducting model rotor icing tests.

Approach

Because no model rotor had ever before been tested in the IRT, it was felt that the best way to successfully conduct this test program was to enlist the aid of the U.S. helicopter manufacturing community to draw upon their collective rotor testing experience. To this end, a Rotor Icing Consortium has been established whose members include representatives of NASA Lewis, Sverdrup Technology Inc., Bell Helicopter Textron Inc., Boeing Helicopters, McDonnell Douglas Helicopters, Sikorsky Aircraft Division of United Technologies, and Texas A&M University. This consortium setup gives several advantages to the overall program in that it maximizes the return from available resources by taking advantage of each company's unique strengths, it maximizes the speed of data and technology transfer to industry, and it encourages closer long-term contact between NASA and industry.

After evaluating several options, the consortium decided that a Sikorsky Aircraft model, the BMTR-1 (also known as the Powered Force Model or PFM), would be the best available candidate for testing in the IRT. This model is a very complex, heavily instrumented model of the Sikorsky Blackhawk helicopter (Fig. 1). Once the test article was selected, the various tasks necessary to prepare for this test were divided among the consortium participants, as illustrated in Table 1. As may be seen, part of NASA Lewis's responsibilities included development of rotor icing test techniques.

It was then decided that the best way to develop rotor icing test techniques prior to the PFM test would be to test a simpler, more rugged model rotor in the IRT first, with which the necessary experience could be gained. An ideal candidate for this initial entry was the OH-58 Tail Rotor Rig, a relatively sturdy and simple rig designed and built in 1980 at NASA Lewis for just such a purpose, although for various reasons it was never actually tested at that time. The rig was refurbished and installed in a test cell where it underwent an extensive checkout prior to its tunnel entry. During this checkout it was

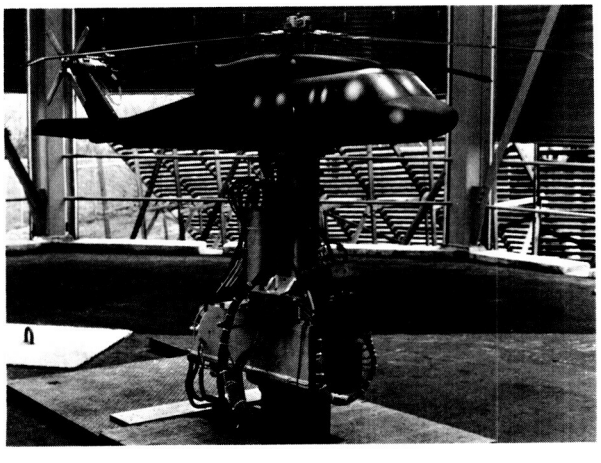

FIGURE 1. - SIKORSKY POWERED FORCE MODEL.

Table 1. Rotor Icing Consortium Responsibilities for Model Rotor Icing Test

Company	Tasks
NASA Lewis RC/ Sverdrup Technology	Project coordinator; provide icing research tunnel; develop icing test techniques
Bell Helicopter	PC-based safety of flight system
Boeing Helicopters	Test plan; analytical modeling
McDonnell Douglas Helicopters	Composite rotor blade design and construction; test support
Sikorsky Aircraft	Prepare and provide model and associated hardware; data acquisition and reduction; test support
Texas A&M University	PC-based data acquisition and reduction system; test support

learned that the first critical speed of the rig was at almost exactly the nominal design rpm of 2600, so for all subsequent runs including the entire wind tunnel test the maximum rotor rpm was limited to 2100 to avoid encountering damaging excitations near the critical speed. The checkout also served to provide baseline data for rig vibration and torque. In the following section a more detailed description of the rig is given, along with a discussion of the various tunnel modifications and other hardware development that took place in order to conduct this test.

Test Apparatus

Tunnel

The Icing Research Tunnel was designed and built in the early 1940's. In 1986 it underwent a major rehabilitation. This upgrade provided faster and more accurate control of tunnel conditions. The spray system was also improved to provide a more realistic range of droplet conditions and better repeatability of the cloud parameters. The IRT is a closed-loop refrigerated wind tunnel. The 4160 hp fan allows airspeed up to 134 m/s (300 mph). It has a 21 000 ton capacity refrigeration heat exchanger which can vary the total temperature from -1.1 to -42 °C (Fig. 2). The spray nozzles currently available can provide droplet sizes from approximately 10 to 40 μm (volume median diameter) with liquid water content (LWC) ranging from 0.2 to 3.0 g/m^3. The tunnel test section is 1.8 m (6 ft) high by 2.7 m (9 ft) wide with viewing capability from the control room.

The model rotor test presented some unusual hurdles to overcome in the tunnel entry. Personnel in the control room or other access/viewing areas to the test section had to be protected from the potential catastrophic failure of the rotating hardware. A set of armor plates on rails was designed to cover the vulnerable tunnel wall areas (Fig. 3). The potential viewing areas not covered by plating (tunnel ceiling and diffuser) were isolated during operation of the rig. A hierarchy of restricted personnel, keyed entrances, and locked start-up systems was also initiated to prevent anyone operating the test hardware while someone was working in the tunnel. The armor plating prevented any viewing of the test sessions so a video system was installed to allow tunnel and test operators safety-related monitoring of the test. A set of 0.635 mm

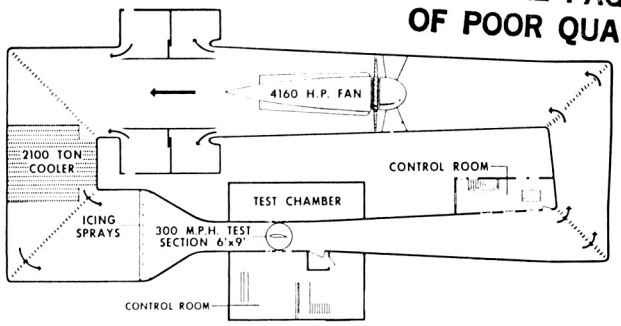

FIGURE 2. - ICING RESEARCH TUNNEL.

FIGURE 3. - IRT TEST SECTION WITH ARMOR PLATING ON THE WALLS.

(0.025 in.) aluminum sheets were placed over the armor plating near the high probability impact areas in line with the rotational field of the tail rotor. The sheets were locked in place over energy absorbing material to allow permanent dents to be made as shed ice left the blades. The dents will be calibrated to calculate the impact energy of the ice producing them.

Model Rotor

The tail rotor assembly was composed of the tail shaft, hub, teetering components, and rotor blades from an OH-58 helicopter. The rotor blades were NACA 0012 airfoils with a chord of 13.3 cm and a span of 73.0 cm. The total diameter of the rotor assembly was 157.5 cm (Fig. 4). This assembly was mated, through an adapter, to a 2.1 m long NASA designed drive shaft. The extended drive shaft allowed the rotor blades to be run in the horizontal plane in the middle of the test section of the IRT while the drive system hardware remained below the tunnel turntable (Fig. 5). There was a hydraulically operated center tube which controlled the collective pitch of the rotor blades. This provided the ability to change blade angle quickly to the desired condition. The drive housing was bolted to the tunnel floor plate via two gimbal pins. For this test the rotor shaft was set at 5° forward tilt to simulate forward flight of a helicopter.

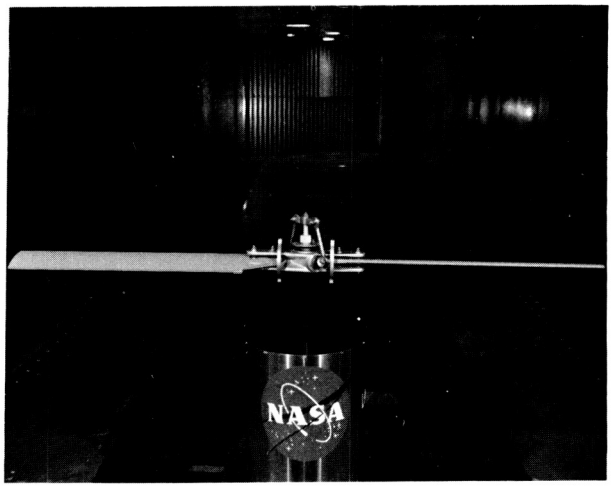

FIGURE 4. - OH-58 TAIL ROTOR ASSEMBLY.

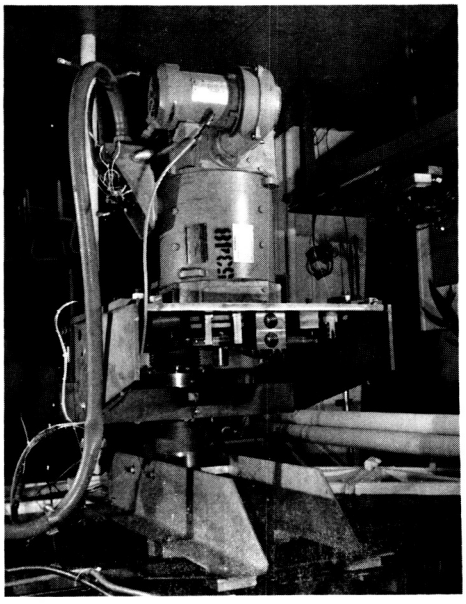

FIGURE 5. - OH-58 MODEL ROTOR DRIVE ASSEMBLY.

The drive shaft was connected to a 40 hp dc electric motor by a five belt pulley system. The motor was controlled by an SCR adjustable speed drive. This drive assembly was chosen because of its flexibility to handle the variable torque loads.

The tail rotor rig was instrumented to provide data collection and safety monitoring capabilities. The critical safety items were rig vibration, temperature, percent drive speed, and the current to the dc motor. The data channels recorded were held to a minimum in keeping with the devlopmental purposes of this tunnel entry. Torque changes were monitored by using a differential measuring device that recorded reaction torque changes from the drive system. A set of redundant speed pick-ups were located on the drive shaft because of the critical nature of

this information. The vibration output was recorded to detail the severity and timing of shedding events with respect to the torque data. Motor hp was calculated and recorded to verify the torque data. Finally, the collective pitch angle was noted to document the rotor blade angles for the specific icing encounters.

All the instrumentation, except the second rotor rpm, was connected to a datalogger system that conditioned the information, converted it to engineering units, and downloaded it to a personal computer (PC) for storage. The datalogger also provided updated information to a CRT screen for review by the model rotor operator. A variable data collection rate was incorporated in the software, but experience indicated a 2 sec interval between data points provided adequate documentation. The redundant speed set-up provided independent observation of rotor rpm in case the datalogger/pc system failed. This allowed a back-up measure of minimum capability to control the rotor speed while the tunnel was being shut down.

Test Setup

The total data acquisition package encompassed the previous instrumentation and datalogger/PC system mentioned plus a number of other measurement and cataloguing techniques. Each run was recorded on video to provide a viewing history of the ice accretions and sheddings. There were two video systems; one for safety monitoring and one that provided close-up movable images of the icing events on a strobe "frozen" blade. The data video system had the capability of traversing the entire diameter of the tail rotor while allowing zoom shots of as small a span as 10 cm of the blade leading edge. There was a 35-mm camera located on the tilt and pan tracking device that the data video system was on. The 35-mm camera was focused on the same close-up viewing area as the video camera. This allowed pictures with greater resolution and clarity to be taken as the icing encounter unfolded.

Throughout each test run the tunnel conditions were monitored. Spray times, temperatures, and plots indicating how quickly the cloud conditions stabilized were recorded. Each shedding event time seen on video, or heard, was also recorded.

Post run information was gathered by taking ice tracings, 35-mm handheld camera shots, visual observations, and ice molds. Heated aluminum blocks with a cut-out contour of the airfoil profile were used to make a clean break in the ice formation. A cardboard template was then held against the ice shape and a tracing made. Measurements of the ice thickness at various chord locations were taken and visual observations about the kind of ice and secondary growth were recorded. Pictures were taken of the full blade, an end view, and any pronounced or unusual ice formations. A mold was taken of one entire blade on the last run of the night on four different occasions. One attempt was unsuccessful, but three molds provided fairly good definition of the ice formations on the blade.

Table 2. Test Matrix

I. Baseline

V_{IRT}, m/s	T_{total}, °C	LWC, g/m^3	MVD, μm	tau, min	Rotor rpm	Collective, deg
31.3	-26.1	--	--	--	1200	2-12, Δ = 2
31.3	-26.1	--	--	--	2100	2-10, Δ = 2
31.3	-15.0	--	--	--	1200	2-12, Δ = 2
31.3	-15.0	--	--	--	2100	2-10, Δ = 2
31.3	-6.7	--	--	--	1200	2-12, Δ = 2
31.3	-6.7	--	--	--	2100	2-10, Δ = 2
53.6	-26.1	--	--	--	2100	2-10, Δ = 2
53.6	-15.0	--	--	--	2100	2-10, Δ = 2
53.6	-6.7	--	--	--	2100	2-10, Δ = 2

II. Cloud Uniformity with Grid Installed

V_{IRT}, m/s	T_{total}, °C	LWC, g/m^3	MVD, μm	tau, min	Rotor rpm	Collective, deg
31.3	-17.8	0.5	15	4.3	----	No blades
31.3	-17.8	.5	15	4.3	1200	4,12
31.3	-17.8	.5	15	4.3	2100	4,9
53.6	-17.8	.5	15	4.3	----	No blades
53.6	-17.8	.5	15	4.3	2100	4,9

III. Rotor Blade Icing

V_{IRT}, m/s	T_{total}, °C	LWC, g/m^3	MVD, μm	tau, min	Rotor rpm	Collective, deg
31.3	-26.1	0.5	15	2	1200	2-12, Δ = 2
31.3	-26.1	.5	15	4	1200	2-10, Δ = 2
31.3	-15.0	.5	15	2	1200	2-12, Δ = 2
31.3	-15.0	.5	15	4	1200	2-12, Δ = 2
31.3	-6.7	.5	15	2	1200	2-10, Δ = 2
31.3	-6.7	.5	15	4	1200	2-10, Δ = 2
31.3	-15.0	.5	15	2	1700	2-8, Δ = 2
31.3	-26.1	.5	15	2	2100	2-10, Δ = 2
31.3	-26.1	.5	15	4	2100	2-10, Δ = 2
31.3	-20.6	.5	15	2	2100	2-8, Δ = 2
31.3	-15.0	.5	15	2	2100	2-10, Δ = 2
31.3	-15.0	.5	15	4	2100	2-8, Δ = 2
31.3	-12.2	.5	15	2	2100	2-6, Δ = 2
31.3	-12.2	.5	15	3+	2100	4,6
31.3	-9.4	.5	15	2-5+	2100	4,6
31.3	-6.7	.5	15	2	2100	2-10, Δ = 2
31.3	-6.7	.5	15	4	2100	2-10, Δ = 2
53.6	-15.0	.5	15	2	2100	2-6, Δ = 2
31.3	-20.6	.4	12	2	2100	2-6, Δ = 2
31.3	-15.0	.4	12	2	2100	2-8, Δ = 2
31.3	-12.2	.4	12	2	2100	2-6, Δ = 2
31.3	-9.4	.4	12	2	2100	2-8, Δ = 2
31.3	-26.1	.25	10	2	2100	2-8, Δ = 2
31.3	-20.6	.25	10	2	2100	2-8, Δ = 2
31.3	-15.0	.25	10	2	2100	2-8, Δ = 2
31.3	-15.0	.25	10	4	2100	2-6, Δ = 2
31.3	-12.2	.25	10	2	2100	2-8, Δ = 2
31.3	-6.7	.25	10	2	2100	2

IV. Rotor Blade Icing with B.F. Goodrich Blades

V_{IRT}, m/s	T_{total}, °C	LWC, g/m^3	MVD, μm	tau, min	Rotor rpm	Collective, deg
31.3	-12.2	0.5	15	3.6	2100	4
31.3	-12.2	.5	15	2.5	2100	6
31.3	-9.4	.5	15	5.4	2100	4
31.3	-9.4	.5	15	4.9	2100	6
31.3	-9.4	.5	15	3.9	2100	4
31.3	-9.4	.5	15	6.8	2100	6
31.3	-12.2	.4	12	6.0	2100	4
31.3	-12.2	.4	12	10.4	2100	6

V. Rotor Blade Icing with B.F. Goodrich Blades and Icephobic

V_{IRT}, m/s	T_{total}, °C	LWC, g/m^3	MVD, μm	tau, min	Rotor rpm	Collective, deg
31.3	-15.0	0.5	15	3.8	2100	4
31.3	-12.2	.5	15	3.7	2100	4
31.3	-9.4	.5	15	6.3	2100	4
31.3	-9.4	.5	15	10.0	2100	4
31.3	-9.4	.4	12	6.7	2100	6
31.3	-12.2	.25	10	10.0	2100	4

At the end of each run a survey of the aluminum sheets was taken and any dents were circled and catalogued with reference information. If the sheets were heavily marked they were replaced by new ones to prevent overstriking the first data points.

A complete matrix of test conditions is presented in Table 2.

Test Procedure

A typical test run consisted of setting the tunnel controls to the desired parameters, bringing the tail rotor speed up to a nominal operating rpm first, and then starting up the tunnel. The overriding safety concern was operating the tail rotor tip speed considerably above the tunnel speed. Once the tunnel conditions were stable the rig operator set the rig rpm and collective pitch and started the PC data acquisition software. The tunnel operator then started the spray. At the end of the run the tunnel rpm was brought to idle and then the tail rotor was shut down. If problems were encountered, the collective pitch and rig speed were decreased to the nominal settings and then the tunnel rpm was returned to zero. After the run was over the researchers entered the test section and documented the results. The assembly was then deiced and conditions set for the next run.

Results

In addition to developing and documenting the test procedures established in this program, much information was gathered regarding the accretion and shedding characteristics of the rotor and the associated effects on rotor performance. This data will be discussed in the following sections which detail the effects of various test parameters on the rotor blade ice accretion and shedding and rotor vibration and torque. Also included are discussions of other items of interest including repeatability of ice shapes, iced rotor torque, shedding, icing cloud uniformity, and ice accretion detail.

Accretion Effects on Rotor Torque

In all cases, ice accretion on the rotor produced a rotor torque rise which was linear with time for a fixed set of rotor and tunnel conditions. The speed with which torque rose with time was dependent upon the specific rotor and tunnel conditions chosen. Below roughly 7° collective, the rate of torque rise with time in icing appeared relatively constant and independent of collective. Over 7° collective, torque rise occurred more rapidly in icing and base (clean) rotor torque showed a significant increase over the base torque at lower collectives. It is believed that at this collective, flow separation is beginning to occur outboard on the rotor blades and the rotor torque then increases correspondingly, and any ice accreted on the blades will then further the torque elevation.

The torque rise rate was also found to be dependent on cloud conditions (lower liquid water content and lower drop size give slower torque rise) and temperature (there is some "worst" temperature at which ice is predominantly glaze and extends to the tip without shedding). Because several different parameters affect the accretion and shedding characteristics of a system, the conditions which produce the highest torque rise rate will vary from one configuration to another. The worst case will most likely occur though at some intermediate temperature which is conducive to glaze ice formation but also is cold enough to produce bonding strengths even in the tip region which are strong enough to hold the ice on the rotating blade. For this particular test that temperature appeared to be in the neighborhood of 5 °F.

Figure 6 presents a typical torque history in a case where multiple sheds occurred. Here torque rose smoothly until shedding occurred, the shed dropped the torque somewhat, and as ice continued accreting on the blade the torque rose again until another shed took place. If the accretion was allowed to continue long enough, an "equilibrium" time would be reached at which shedding and accretion would roughly balance each other out. Torque would then level off at some final equilibrium value.

Accretion Effects on Vibration

As expected, ice accretion on the rotor blades tended to increase vibration due to added mass on the blades and distortion of the flow field around the blades' leading edges. Because the accretion was always very symmetric, vibration rise before shedding was gradual. Occasionally, depending on collective primarily and also temperature, vibration rose to high enough levels to necessitate stopping the spray before any shedding occurred. Otherwise vibration would rise gradually until shedding took place. At this time the vibration would either decrease if the blades shed relatively symmetrically or increase if the shedding occurred on only one blade. The direction and magnitude of the vibration change at shedding was generally sufficient to indicate symmetric or asymmetric shedding to the operator without any visual indicator

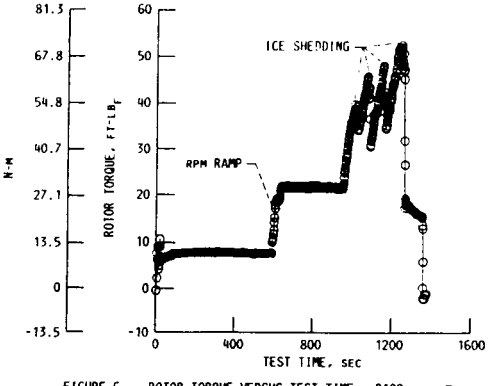

FIGURE 6. - ROTOR TORQUE VERSUS TEST TIME. 2100 RPM, T = 5.4 MIN, 15 μM, 31.3 M/S, -9.4 °C, .5 g/m^3, θ_{75} = 4°.

required. Using previously established guidelines a safe vibration limit of 0.76 cm/sec was set. Whenever vibration met or exceeded this level longer than instantaneously the test conductor would have the spray stopped and the rotor loading decreased by dropping the collective and rpm to some lower values.

Upper radial velocities were the most active vibration channels and were most heavily monitored during icing. The other two vibration channels, upper thrust and lower radial, exhibited negligible movements under all conditions. So the primary effect of ice accretion and shedding appeared to be a more pronounced in-plane rotor vibration. Figure 7 shows a typical iced rotor vibration history.

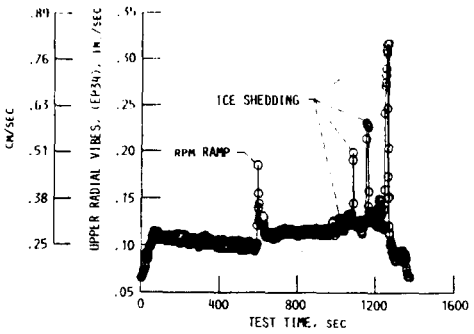

FIGURE 7. - UPPER BEARING VIBRATION VERSUS TEST TIME. 2100 RPM, T = 5.4 MIN, 15 μM, 31.3 M/S, -9.4 °C, .5 g/m^3, θ_{75} = 4°.

Ice Shape Repeatability

Overall ice shape repeatability was found to be very good in this test. For a given set of rotor and tunnel conditions and at a given radial location tracings of the two-dimensional shape were made and compared to obtain a measure of this repeatability. These two-dimensional shapes were found to agree best at colder temperatures where the formation was of a rime nature and was fairly smooth and easily traceable. The ice tracings tended to vary more at warmer temperatures due not necessarily to actual variation in the shapes but primarily due to difficulty in obtaining accurate tracings of these relatively small but complex geometries. Even with the tracing difficulties however repeatability can be seen to be quite good at these warmer temperatures.

Figure 8 illustrates the quality of ice shape repeatability for one particular condition which was run several times during the test. As may be seen the ice shape at the measurement location was of a glaze nature with a slight double horn shape and some degree of roughness and secondary ice formation behind the primary shape. In making the cut in the ice to get to a two-dimensional tracing, often much of the detail in the secondary formations was lost due to melting when the cut was made, and some of the roughness and finer details of the primary shape were also affected by partial melting during the cut. Even with some loss of detail though it can be seen that the ice shapes tended to repeat quite well from run to run. More care was taken later in the test to preserve the roughness and secondary formation detail so the final two tracings show more detail and better illustrate the actual ice shape which existed at this condition throughout the test program. This same degree of two-dimensional ice shape repeatability was seen at all other test conditions as well.

In addition to the two-dimensional tracings, a measure of ice shape repeatability was also available from photographs and post-run observations of the overall characteristics of the ice in each run. Especially at the -15.0 °C intermediate test temperature, the ice could be seen to transition from rime to glaze at some point or zone along the blade and this transition location was found to be repeatable within approximately 5 percent for a given set of conditions. Because

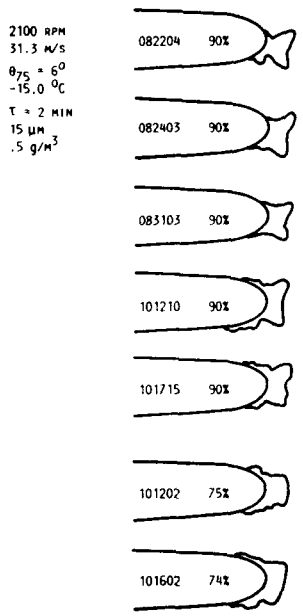

FIGURE 8. - ICE SHAPE REPEATABILITY.

of the gradual nature of the transition it is difficult to better quantify the transition location than to state a zone in which transition seemed to always occur for a given set of conditions. For the -15.0 °C cases run, at a liquid water content of 0.5 g/m^3 and a median droplet diameter of 15 μm, this transition zone appeared to be between 60 and 75 percent span. Inboard of this the primary ice formation was of a smooth, whitish nature and outboard of this region the ice had become clear and significantly rougher. Other sets of conditions also exhibited the same quality of repeatability in terms of transition zones.

Also measured after each run were the upper and lower blade surface icing extents in order to quantify chordwise impingement limits. These measurements were found to be very repeatable for a given set of conditions, especially at the colder temperatures where secondary ice roughness and feathers did not exist or were very small. As temperature increased it became increasingly

more difficult to specify a certain impingement limit due to the normal variations in roughness and feathers spanwise on the blade. Even so, the degree of impingement limit repeatability was judged to be quite good for all operating conditions.

One final measure of the ice shape was the leading edge thickness of ice. This measurement was made at the leading edge at the location which was judged to be the stagnation point for that run. This quantity too was found to be very repeatable for a given set of conditions throughout the test program.

Ice Shedding Repeatability

Ice shedding occurred to a limited degree in this test program, primarily at the warmer test temperatures. At the coldest test temperature, -26.1 °C, no shedding took place in any of the runs. At the warmest temperature tested, -6.7 °C, and at the densest cloud conditions tested (15 μm, 0.5 g/m^3) the ice remained adhered to the blade inboard of roughly 85 percent span and outboard of that accreted in very small amounts and then shed several times during the run, so that at the end of the run there typically would be some slight amount of residual ice outboard of the 85 percent station with a primary glaze formation inboard of that. At the lightest cloud conditions tested, 10 μm and 0.25 g/m^3, no ice formed at all on the blades at -6.7 °C.

The -15.0 °C temperature data provided the most insight into the ice shedding repeatability issue. For the 15 μm and 0.5 g/m^3 condition, ice accreted over the entire blade leading edge and then typically shed from somewhere in the outer 30 percent of the blade. Twenty runs were performed at this condition for an icing time of 2 min each at various collective pitch settings, and of those 20 runs ice shedding occurred in 15 of the runs. In 8 of these 15 shedding runs, the ice shed asymmetrically and in 7 it shed symmetrically (within 10 percent on both blades).

In all of the shedding runs at -15 °C, shedding did not occur until just after the spray was stopped. It is postulated that the sudden change in turbulence at the end of the spray was at least partly responsible for the production of ice shedding at that point. In a few cases, shedding did not occur until either the rotor collective or tunnel velocity were dropped at the end of the run. Rotor drive system limitations did not allow for a long enough icing exposure to produce shedding during the icing spray at this temperature. Although the shedding at this condition appeared to in all cases be induced by some sudden change in the local rotor flowfield, the shedding data acquired did appear to be repeatable in terms of radial location and nature of the shedding process. When the cloud conditions were changed to 10 μm and 0.25 g/m^3 at this same temperature, no shedding took place due to the smaller mass of ice accreted by the thinner cloud and the resulting decreased centrifugal force on the ice.

Temperature Effects

A wide range of tunnel total temperatures from -26.1 to -6.7 °C were run in this test. This range permitted examination of the rotor ice accretion characteristics from the rime to mixed to glaze ice regimes. In so doing, temperature was found to have a significant effect on the rotor ice accretion and shedding characteristics.

Tunnel total temperature combined with the rotational effect of kinetic heating on the local blade temperatures were found to influence both ice type and transition location from rime to glaze ice. In addition, the existence and size of secondary ice formations typically in the form of ice feathers were affected by the local temperature. Figure 9 illustrates the change in ice

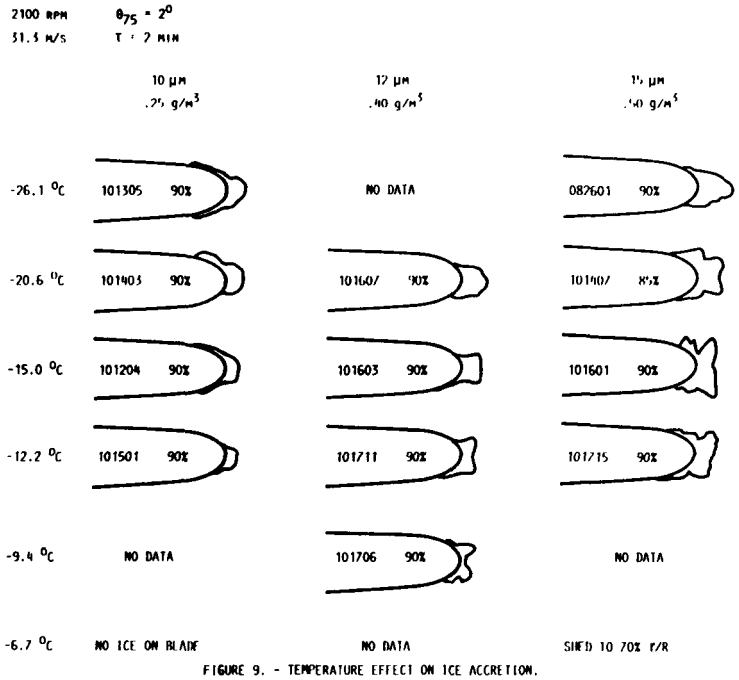

FIGURE 9. - TEMPERATURE EFFECT ON ICE ACCRETION.

type at a given location and condition over a range of tunnel total temperatures.

Temperature was found to have a significant effect on iced rotor torque for a given set of test conditions. The effect of temperature is felt through variation in the rotor ice shapes which different temperatures cause. At the coldest temperature tested, -26.1 °C, the ice was all of a rime nature, giving only a relatively minor distortion to the leading edge shape. Consequently the resulting torque rise was generally the least severe for a given condition at the three primary test temperatures.

At -15.0 °C, the ice type varied radially from rime inboard to glaze outboard and because of the presence of some glaze ice on the blades the torque rise was more severe than at the colder temperature. At this temperature maximum torque varied somewhat due to ice shedding which was often not repeatable.

Finally at -6.7 °C the ice had become predominantly glaze over most of the blade. Because of the increased local temperature in the outer portion of the blade, ice did not form on the outer 15 to 20 percent of the blade at this temperature and this served to make the torque rises typically less severe than their counterparts at -15.0 °C.

Liquid Water Content & Drop Size Effects

Variations in cloud liquid water content (lwc) and median volumetric droplet diameter (mvd) were found to produce a measurable change in the accretion and shedding characteristics of the rotor blade ice formations. Primarily for reasons of trying to obtain stable spray conditions the liquid water content and drop size were always varied in tandem in this test. This precluded determination of the effect of each specific parameter alone on the resulting ice shape but still yielded insight into the changes which cloud parameters had on the resulting rotor ice shapes.

Three different lwc/mvd combinations were run in this test (10 μm and 0.25 g/m^3, 12 μm and 0.40 g/m^3, and 15 μm and 0.50 g/m^3). Each produced markedly different accretions for a given set of conditions as Fig. 8 shows for one sample case at three different temperatures. Increasing the lwc/mvd had the effect of further encouraging glaze ice formation at a given temperature and given radial location.

In conjunction, varying the lwc/mvd combination was also found to affect the location of the transition region from rime to glaze ice on the blade. As the lwc/mvd were decreased at a given condition, the rime-to-glaze transition zone moved outboard on the blade. For example, at the -15.0 °C case shown in Fig. 10 the transition point was observed to be at approximately the 45 to 50 percent radial location for the 0.5 g/m^3 and 15 μm condition. At 0.4 g/m^3 and 12 μm, the transition point had moved out to roughly the 80 percent station, and at 0.25 g/m^3 and 10 μm the blade ice shape was fully rime with no transition to glaze observable.

Cloud liquid water content and drop size were seen to have a significant effect on rotor torque and vibration by influencing the size and type of ice which formed on the rotor blades. Each of the three sets of cloud conditions produced markedly different ice shapes and therefore markedly different torque levels for a given rotor operating condition and temperature.

As Fig. 11 illustrates, going from the clean blades to a 2 min icing spray at a liquid water content of 0.25 g/m^3 and median droplet diameter of 10 μm, only a very small change in torque was produced. Further raising the cloud density to 0.4 g/m^3 and the droplet diameter to 12 μm yielded consistently higher torque values, raising the torque by a roughly constant 16.3 N-m. An even more substantial torque rise was produced by going to a liquid water content of 0.5 g/m^3 and droplet diameter of 15 μm. Here the torque was found to rise by a roughly constant 31.8 N-m at each collective.

RPM Effects

Rotor rpm was found to have a substantial effect on the nature of the ice which formed on the blades under a given condition. Increasing rpm had the effect of increasing the local velocity at some radial station which then encouraged a more glaze-oriented formation than did the lower speeds. This in turn had the effect of shifting the rime-to-glaze ice transition zone further inboard on the blade as rpm was increased. Figure 12 illustrates this rpm effect for a given set of conditions.

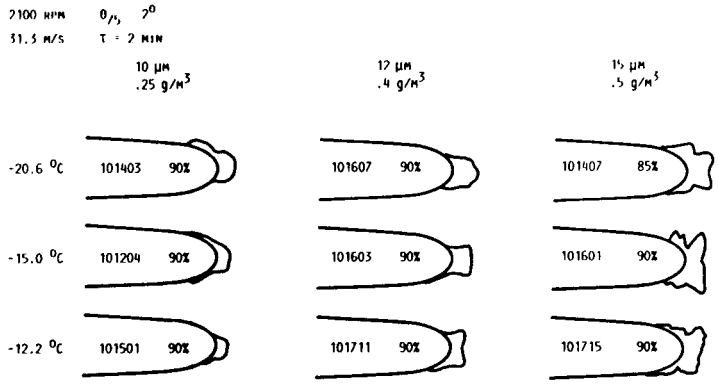

FIGURE 10. - LWC AND DROP SIZE EFFECT ON ICE ACCRETION.

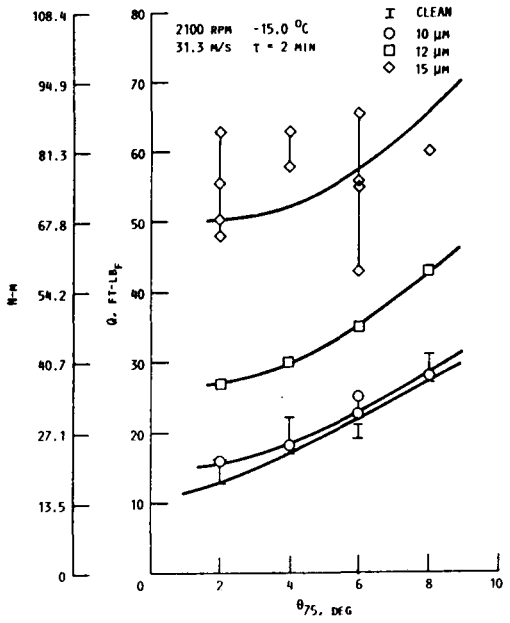

FIGURE 11. - IWC/DROPLET SIZE EFFECT ON TORQUE.

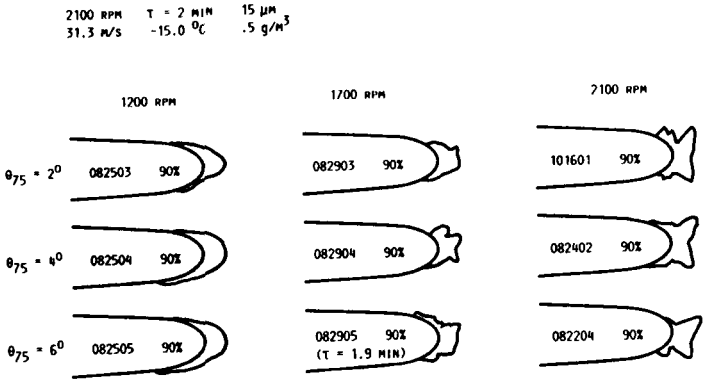

FIGURE 12. - RPM EFFECT ON ICE ACCRETION.

At the lowest test rotor speed of 1200 rpm, the ice which formed at 15 μm and 0.5 g/m^3 was a smooth, whitish rime in nature over the entire span of the blade. Behind this rime formation were ice feathers which were generally small but increased in size and roughness as they progressed outboard on the blade.

Operation at 1700 rpm at the same cloud conditions and icing time yielded a somewhat different spanwise character to the ice. At this rpm, the inboard rime ice transitioned into a glaze formation at roughly the 80 to 85 percent radial location. Here the ice became clearer and rougher and started to develop the characteristic glaze double-horned formation. Heavy feathers were noted behind the primary ice formation at this rotor speed.

Runs at a still higher rpm of 2100 continued the trend toward more glaze ice formation on the blade. At this rpm the transition zone from rime to glaze was seen to shift further inboard to roughly the 70 to 75 percent radial location. The ice was fully of a glaze nature at the tip and the feathers which were present to the tip at 1700 rpm now typically ended at 75 to 85 percent span as the flow became further separated behind the main formation.

In terms of shedding, rpm was again seen to have a significant effect as expected. No shedding occurred in any of the runs at 1200 rpm since the centrifugal forces were simply too low to expel the amounts of ice which accreted on the blades. Likewise at 1700 rpm no shedding was noted in any of the runs. Finally at 2100 rpm shedding began to occur as the centrifugal forces increased to a level where they were significant in relation to the ice bonding forces.

Unfortunately even at this rpm the shedding capability of the rig could not be fully investigated due to the drive system power limitation which existed. Much of the ice shedding which occurred came about seconds after the end of the spray when the air turbulence suddenly changed as the spray stopped, or shedding also often occurred during slowdown of the tunnel or lowering of the collective at the end of the run. There were a few cases where shedding during the spray did occur, but most often the ice accreted on the blades produced such a torque rise that the rig drive system limit was reached before the

ice mass was great enough to make the centrifugal forces adequately sizeable to induce shedding.

Cloud Uniformity

An area of concern prior to the test was the effect of the rotor on the motion of the incoming spray cloud. It was felt that rotor downwash action may tend to draw the cloud downward as it approached the rotor such that the rotor would not be immersed completely in the cloud but rather would sweep the cloud under the rotor. A metal grid with 0.64 cm diameter bars spaced 15.2 cm apart vertically and horizontally was placed 45.7 cm in front of the rotor disk and ice accretion patterns on the grid were examined to ascertain the effect of the rotor on the cloud. The rotor was then operated in icing conditions (-17.8 °C, 15 μm, 0.5 g/m^3, 31.3 m/s) at its nominal operating rpm in both low (collective = 4°) and high (collective = 9° to 12°) loading conditions. Comparison of grid ice accretion patterns in these runs with baseline ice accretion patterns taken with the rotor blades removed showed no significant difference between the baseline and spinning rotor cases for both high and low rotor loadings. This indicates a minimal effect of rotor downwash on incoming cloud position and visual observation of the cloud motion also supported the belief that the rotor was in all runs sufficiently immersed in the cloud to properly represent an actual icing encounter.

Close-Up Detail of Ice

Visual post-run observation of the ice shapes produced by a variety of conditions gave some insight into the nature of the ice accretion process on the rotor blades. In general the rotor ice shapes had a distinct three-dimensional character, especially in the outboard regions where centrifugal force was highest. Stria could be seen in most of the ice shapes and these lines became less vertical and more spanwise-oriented as they progressed out the blade span (Figs. 13 and 14). Inboard of roughly 30 to 50 percent radius the stria generally became almost vertical with respect to span, indicating that centrifugal forces had a negligible influence there. The radial location where the stria became vertical shifted from run to run depending on the particular conditions of each run.

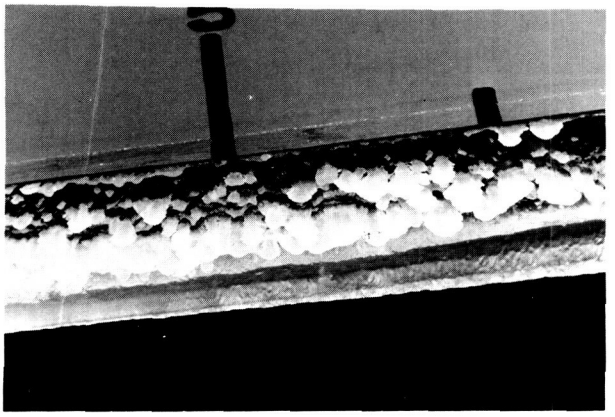

FIGURE 13. - CLOSE-UP DETAIL OF ICE FEATHERS AND PRIMARY FORMATION. 2100 RPM, τ = 3.6 MIN, 15 μM, 31.3 M/S, -12.2 °C, .5 g/M^3, θ_{75} = 4°.

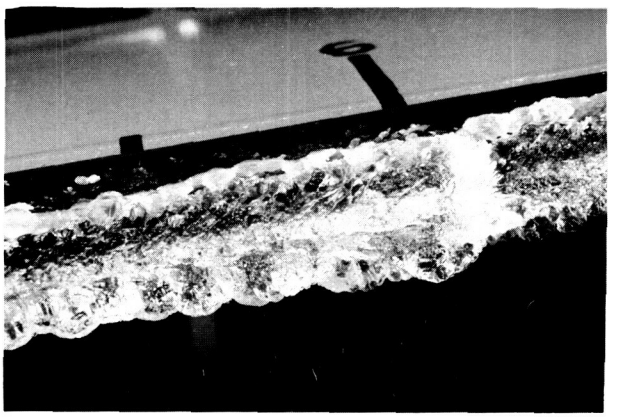

FIGURE 14. - CLOSE-UP DETAIL OF LEADING EDGE ICE FORMATION. 2100 RPM, τ = 5.4 MIN, 15 μM, 31.3 M/S, -9.4 °C, .5 g/M^3, θ_{75} = 4°.

Observation of the ice departing from the blades in conjunction with post-run examination of the remaining rotor blade ice shapes provided insight into the mechanics of the rotor ice shedding process. Typically a chordwise crack would form in the ice at some radial station and once that crack had fully developed the ice tensile strength decreased to zero. At this time, if the centrifugal force on the outboard ice piece was sufficiently large to overcome the ice-blade bond the ice would exit the blade in a radial direction. Figure 15 shows a post-run photo of a blade on which several sheds have occurred during the run.

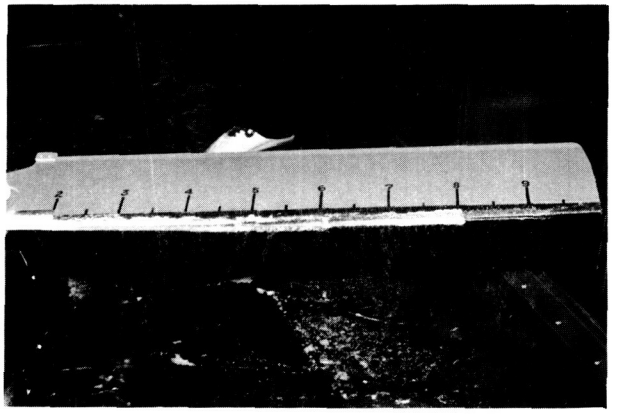

FIGURE 15. - LEADING EDGE ICE FORMATION. 2100 RPM, τ = 5.4 MIN, 15 μM, 31.3 M/S, -9.4 °C, .5 g/M^3, θ_{75} = 4°.

Shed Ice Impact Energy Study

An attempt was made during this test to quantify the impact energy of the ice which was shed from the blades using the procedure outlined in the test apparatus and procedure sections of this paper. Impact dents were successfully obtained in several icing runs but efforts have not yet been initiated to determine the ice geometry and impact energy associated with each dent. It is hoped that this information, once acquired, will serve to enhance knowledge in the area of structural tolerance to shed ice strikes which then directly relates back to de-/anti-icing system design.

Summary

An OH-58 Tail Rotor Rig has been operated in the NASA Lewis Icing Research Tunnel to study the nature of the ice accretion process on a rotating system and the ensuing effect which this ice accretion has on the rotor's performance. Procedures for testing a model rotor in an icing wind tunnel environment were established and refined and an extensive iced rotor performance data base was also created. With this experience now in hand, the 1989 IRT test of the Sikorsky PFM can be conducted more productively.

Since the testing of the OH-58 rig in the IRT represented the first U.S. icing wind tunnel testing of a model rotor, there were many unknowns which needed to be addressed in composing and executing the test. Items such as coordination of model and tunnel operation, observation and documentation of the rotor ice accretion and shedding, and safety and emergency procedures were given special attention. Also of concern was the manner in which the rotor would react to the addition of ice to and expelling of ice from the rotor blades and the controllability of the model rotor under these circumstances. Rotor vibration became a problem only in some cases where ice shed asymmetrically from the blades or when excited by passing through a rig resonant frequency. Rotor rpm and collective controls were never jeopardized by ice accretion or shedding.

A substantial and unique rotor ice accretion and performance data base was acquired in this test. The rotor blade ice shapes were found to be quite repeatable for a given set of conditions and this then yielded iced rotor torque values which were also repeatable up to the onset of shedding. Although the test rotor rpm precluded obtaining as much shedding data as was originally planned, the runs in which ice did shed showed the radial extent of the nonshed ice to be relatively repeatable but the shed times, locations, and quantities of ice shed exhibited substantial variations from run to run. In many instances it was possible to observe the development and occurrence of an ice shedding episode and these observations provided much insight into the rotor ice shedding process.

Conclusions

The successful execution of the OH-58 Tail Rotor Rig test in the NASA Lewis Icing Research Tunnel has demonstrated the viability of using a model rotor to obtain meaningful rotor icing accretion and performance data. Data gathered in this test was repeatable and comparable to full-scale flight test data in terms of the nature of the accretions and their effect on rotor performance. Techniques for testing of a model rotor in a wind tunnel icing environment were developed and will now serve to enhance the future successful testing of other models of rotating systems in icing.

As a first-entry test, the OH-58 program was not able to address in detail some aspects of the rotor ice accretion and shedding process. For example, blade surface finish is acknowledged to be an important factor in ice accretion and adhesion and although the B.F. Goodrich portion of this test showed that altering the blade surface finish did have a significant effect on the resulting ice accretion and shedding, a quantification of the degree of change in the ice accretion and bonding as a function of blade surface finish was not performed in this test program.

No attempt was made in this test to directly scale the test conditions to full-scale. Cloud mvd was selected to provide the smallest measurable drop size to roughly simulate the rotor chord to drop size ratio typically found in a full-scale situation but strict scaling relations were not followed. In future testing however it will be desirable to not only provide nonscaled icing data for analytical method development and validation as this test did, but to also collect data which can be more closely scaled to full-scale conditions to directly compare with flight test results.

One other element of the accretion and shedding process which was not addressed in this program was the effect of blade flexure on these items. Much unlike a typical full-scale rotor blade, the OH-58 tail rotor is a rigid blade whose dynamics are quite different from those of a normal main rotor so that effects of blade bending were not considered in this test. In order to properly simulate a full scale main rotor configuration it will be necessary to eventually construct and test dynamically scaled model rotor blades in future testing.

The complexity of the rotor ice accretion and shedding process will require a substantial investment of time and money and continued development of innovative testing methods to more fully address and understand the nature of the phenomena involved. Many issues remain to be confronted as previously mentioned. The testing of the OH-58 Tail Rotor Rig though represents a positive and crucial first step in this effort.

References

1. Abbott, W.Y., Belte, D., Williams, R.A., and Stellar, F.W., "Evaluation of UH-1H Hover Performance Degradation Caused by Rotor Icing," USAAEFA Report 82-12, Aug. 1983. (Avail. NTIS, AD-A141252.)

2. Abbott, W.Y., Linehan, J.L., LockWood, R.A., and Todd, L.L., "Evaluation of UH-1H Level Flight Performance Degradation Caused by Rotor Icing," USAAEFA Report 83-23, July 1984.

3. Lee, J.D., Harding, R., and Palko, R.L., "Documentation of Ice Shapes on the Main Rotor of a UH-1H Helicopter in Hover," NASA CR-168332, 1984.

4. Hanson, M.K. and Lee, J.D., "Documentation of Ice Shapes on the Main Rotor of a UH-1H Helicopter in Level Flight," NASA CR-175088, 1986.

5. Korkan, K.D., Cross, E.J., Jr., and Cornell, C.C., "Experimental Study of Performance Degradation of a Model Helicopter Main Rotor with Simulated Ice Shapes," AIAA Paper 84-0184, Jan. 1984.

6. Korkan, K.D., Cross, E.J., Jr., and Miller, T.L., "Performance Degradation of a Model Helicopter Rotor with a Generic Ice Shape," Journal of Aircraft, Vol. 21, No. 10, Oct. 1984, pp. 823-830.

7. Guffond, D.D., "Icing and De-icing Test on a 1/4 Scale Rotor in the ONERA SIMA Wind Tunnel," AIAA Paper 86-0480, Jan. 1986.

NASA
National Aeronautics and Space Administration

Report Documentation Page

1. Report No.	2. Government Accession No.	3. Recipient's Catalog No.
NASA TM-101978		

4. Title and Subtitle	5. Report Date
Icing Research Tunnel Test of a Model Helicopter Rotor	6. Performing Organization Code

7. Author(s)	8. Performing Organization Report No.
Thomas L. Miller and Thomas H. Bond	E-4677
	10. Work Unit No. 505-68-11

9. Performing Organization Name and Address	11. Contract or Grant No.
National Aeronautics and Space Administration Lewis Research Center Cleveland, Ohio 44135-3191	13. Type of Report and Period Covered Technical Memorandum
12. Sponsoring Agency Name and Address	14. Sponsoring Agency Code
National Aeronautics and Space Administration Washington, D.C. 20546-0001	

15. Supplementary Notes

Prepared for the 45th Annual Forum and Technology Display sponsored by the American Helicopter Society, Boston, Massachusetts, May 22-24, 1989. Thomas L. Miller, Sverdrup Technology, Inc., NASA Lewis Research Center Group, Cleveland, Ohio 44135; Thomas H. Bond, NASA Lewis Research Center.

16. Abstract

An experimental program has been conducted in the NASA Lewis Research Center Icing Research Tunnel (IRT) in which an OH-58 tail rotor assembly was operated in a horizontal plane to simulate the action of a typical main rotor. Ice was accreted on the blades in a variety of rotor and tunnel operating conditions and documentation of the resulting shapes was performed. Rotor torque and vibration are presented as functions of time for several representative test runs, and the effects of various parametric variations on the blade ice shapes are shown. This OH-58 test was the first of its kind in the United States and will encourage additional model rotor icing tunnel testing. Although not a scaled representative of any actual full-scale main rotor system, this rig has produced torque and vibration data which will be useful in assessing the quality of existing rotor icing analyses.

17. Key Words (Suggested by Author(s))	18. Distribution Statement
Helicopter rotor; Icing; Ice accretion; Ice shedding; Rotor ice shapes; Rotor torque	Unclassified – Unlimited Subject Category 07

19. Security Classif. (of this report)	20. Security Classif. (of this page)	21. No of pages	22. Price*
Unclassified	Unclassified	14	A03

NASA FORM 1626 OCT 86

*For sale by the National Technical Information Service, Springfield, Virginia 22161